International Journal of Smart Home
Vol. 10, No. 4 (2016), pp. 167-182
http://dx.doi.org/10.14257/ijsh.2016.10.4.16

A Novel Non-Line of Sight Identification Algorithm in the 60 GHz Wireless Communication Systems

Xiaolin Liang[1], Hao Zhang[1,2], Tingting Lu[1], Xuerong Cui[3] and T. Aaron. Gulliver[2],

[1]*College of Information Science and Engineering, Ocean University of China, Qingdao, 266100, China;*
[2]*Department of Electrical and Computer Engineering, University of Victoria, Victoria V8W 3P6, Canada*
[3]*Department of Computer and Communication Engineering, China University of Petroleum (East China), Qing Dao, China*
[1]*xiaolin87liang@163.com,* [2]*zhanghao@ouc.edu.cn,*
[3]*lvtingting33@163.com,* [4]*cuixuerong@163.com*
[5]*agullive@ece.uvic.ca*

Abstract

The major problem of indoor localization is the presence of non-line-of-sight (NLOS) channels. In order to perform the NLOS identification, in this paper, we propose a novel NLOS identification technique based on the ratio values of kurtosis and minimum slope of energy block of the received signal using energy detector. In particular, the IEEE 802.15.3c 60 GHz channel models are used as examples and the above statistics is found to be explained in detail. The simplicity of the proposed approach lies in the use of the parameters of the energy-based time of arrival (TOA) estimation algorithm. The CM1 (LOS) and CM2 (NLOS) channel models of the standard IEEE 802.15.3c channel models are used. Numerical simulations results show that the correct identification of channel models with the proposed approach is better than with the multipath channel statistics based approach.

Keywords*: NLOS identification, kurtosis, minimum slope, 60 GHz, energy detector, IEEE 802.15.3c*

1. Introduction

The location of a mobile terminal (MT) can be estimated using different parameters of a received signal, such as the time-of-arrival (TOA), angle-of-arrival (AOA), and/or the received signal strength (RSS). Impulse Radio (IR) - 60 GHz has a great potential for accurate ranging and localization systems due to its very wide bandwidth and capability in resolving individual multipath components [1–6]. Therefore, the TOA of the received signal can be estimated with high accuracy for 60 GHz systems if the first arriving path has been identified precisely. One of the major challenges for localization systems is the mitigation of non-line-of-sight (NLOS) effects. If the direct path between a fixed terminal (FT) (An FT is usually a base station in a cellular network or an anchor node in a sensor network.) and the MT is being obstructed, the TOA of the signal to the FT will be delayed, which introduces a positive bias. Using such NLOS TOA estimates during the localization of the MT position may significantly degrade the positioning accuracy. Hence, FTs that are under the NLOS condition have to be identified and their effects have to be mitigated.

The NLOS identification and mitigation techniques have been discussed extensively in the literature, but mainly within the cellular network framework [7–13]. For example, in [7], skewness of the ranging measurements is compared with the threshold for NLOS identification, where the measurement noise variance is assumed to be known. In [8], a

ISSN: 1975-4094 IJSH

decision-theoretic NLOS identification framework is presented, where various hypothesis tests are discussed for known and unknown probability density functions (PDFs) of the TOA measurements. Guvenc *et al*. [9 -13] used mean excess delay, root mean square (RMS) delay, and kurtosis of multipath channel as NLOS identification metrics. When the statistics of Kurtosis, mean excess, and RMS delays are priori known, likelihood ratio tests can be performed for hypothesis selection. Another method was proposed by Heidari *et al*. [10]. They tried to find the first detected path of the received signal as a peak of the filtered Channel Impulse Radio. As similar to the previous method, this technique also used joint likelihood function using the mean excess delay τ_{med}, total received power P_{tot} and the hybrid of the power of the first detected path and TOA of the first detected path ξ_{hyb}

Venkatesh *et al.* [11] identified the channel based on TOA, RSS, and RMS delay spread (RDS) of the received signal. The conditional distributions of the TOA, RSS, and RDS estimates are functions of the distance and the channel state. Provided that the physical distance between the transmitted and receive nodes is known exactly, the state of the channel can be identified by comparing the likelihood values for each of the estimates (TOA, RSS, and RDS), conditioned on the distance. Shimizu *et al*. [12] performed intensive measurements of path-loss and delay-profile characteristics of LOS and NLOS environments in a suburban residential area. Based on their analysis, they found that the delay spread was dependent on distance, and the NLOS delay spread was found to be several times larger than that of the LOS case. The skewness of delay spread for the NLOS cases ranged from 80 to 200 ns, which was an order of magnitude larger than that of the LOS case.

To the best of authors' knowledge, the LOS/NLOS identification of 60 GHz signal under the IEEE 802.15.3c channel model hasn't been identified. In this paper, we propose a new LOS/NLOS identification approach for the IR-60 GHz signal, which is based on the minimum slope and kurtosis of energy block of the received signal using energy detector. Firstly, we use the energy detector TOA Estimation algorithm for the estimation the TOA. Secondly, we characterize the minimum slope and kurtosis of the energy block of the received signal. Finally, we use a threshold test for LOS/NLOS identification.

The remainder of this paper is organized as follows. Section II describes the signal and channel model. Section III describes LOS/NLOS identification approach and Section IV presents the results of the numerical simulations. The concluding remarks are given in section V.

2. System Model

Currently, there are two important standards that have been developed for 60 GHz wireless communications systems, IEEE 802.15.3c and IEEE 802.11ad [14-15]. In this paper, the channel models in IEEE 802.15. 3c standard are used because it is specifically designed for Wireless Personal Area Networks (WPAN) and thus encompasses typical indoor environments. Further, these are the most widely employed models for 60 GHz systems. The IEEE 802.15.3c standard was the first developed for high data rate short-range wireless systems. The physical layer was designed to support the transmission of data within a few meters at a maximum data rate of 2 Gbps. These models have been developed for communications in the frequency band 57 to 66 GHz in indoor residential, indoor office and library environments (with differences largely due to the LOS and NLOS characteristics) [16-20].

In this paper, a Pulse Position Modulation Time Hopping (PPM-TH) 60 GHz signal is employed for ranging purposes. The propagation delay $\hat{\tau}$, between the transmitter and receiver is estimated for use in localization.

2.1. 60 GHz Signal

The PPM-TH 60 GHz signals have a very short duration (typically 100 picoseconds or less), and can be expressed as

$$s(t)=\sum_{-\infty}^{\infty} p\left(t-jT_s-C_jT_c-a_j\varepsilon\right) \tag{1}$$

where T_s is the symbol time. The Time Hopping (TH) code represented by C is a pseudorandom integer-valued sequence which is unique for each user to limit multiple access interference, and T_c is the chip time. The PPM time shift is ε so that if a_j is 1, the signal is shifted in time by ε, while if a_j is 0, there is no shift. Many pulse shapes have been proposed for 60 GHz systems. In this paper a Gaussian pulse is employed which is multiplied by the carrier signal to give

$$p(t)=\frac{\sqrt{2}}{\alpha}\exp\left(-2\pi\frac{t^2}{\alpha^2}\right)\cos\left(2\pi f_c t\right) \tag{2}$$

where α is the shape factor and f_c is the carrier frequency which here is $f_c=60$ GHz. A smaller shape factor results in a shorter duration pulse and a larger bandwidth.

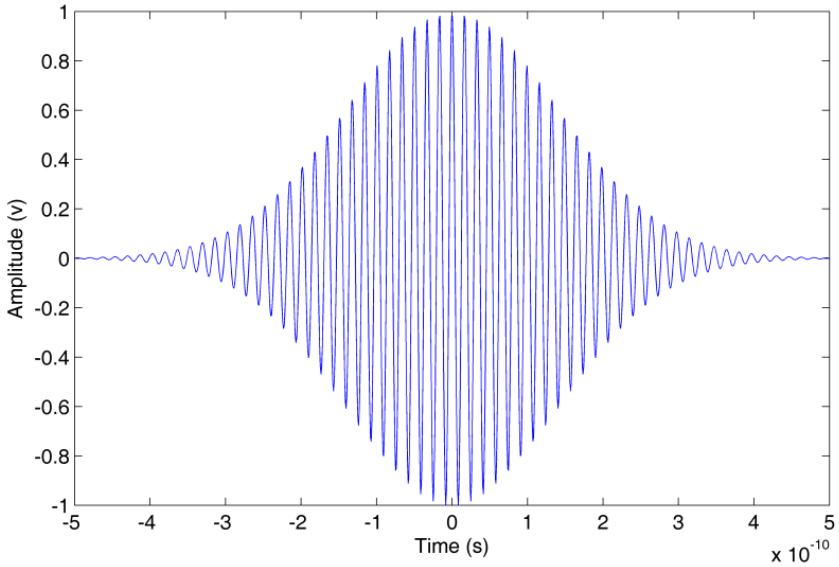

Figure 1. Waveform of 60GHz Signal

2.2. Signal Shift and Path Loss

The path loss is defined as the ratio of the received signal power to the transmit signal power and it is very important for link budget analysis. Unlike narrow-band system, the path loss for a wide-band system such as mm-wave system is both distance and frequency dependent. In order to simplify the models, it is assumed that the frequency dependence Path Loss is negligible and only distance dependence path loss is modeled. The signal path loss, which depends on the propagation distance and the channel (IEEE802.15.3c), is described by

$$PL(d)[dB]=PL_0+10\cdot n\log_{10}\left(\frac{d}{d_0}\right)+X_\sigma[dB];\ d\geq d_0 \tag{3}$$

where d_0 and d denote the reference distance, and distance respectively and n is the path loss exponent for mm-wave based measurements ranges. X_σ is that the unit dB, with mean zero and variance σ_s for a Gaussian random variable. Table 1 summarizes the values of n, PL_0, σ_s for different environments and scenarios.

Table 1. Values of n, PL_0, σ_s for Different Environments and Scenarios

environments	n	PL_0	σ_s
indoor residential (LOS)	1.53	75.1	1.50
indoor residential (NLOS)	2.44	86.0	6.20
indoor office (LOS)	1.16	84.6	5.40
indoor office (NLOS)	3.74	56.1	8.60

The signal shift can be expressed as

$$t = dt * floor\left(\left(d / c\right)/dt\right) \tag{4}$$

where d denotes the distance between the transmitter and receiver, dt is the sampling period and c is the speed of light which is 299792458m/s in the air.

2.3. Multipath Fading Channel

The received signal can be written as

$$r\left(t\right) = \sum_{n=1}^{N} \alpha_n p\left(t - \tau_n\right) + n\left(t\right) \tag{5}$$

where N is the number of received multipath components, α_n and τ_n denotes the amplitude and delay of the nth path respectively, $p(t)$ is the received 60 GHz pulse and $n(t)$ is Additive White Gaussian Noise (AWGN) with zero mean and two sided power spectral density N0/2. Equation (5) can be rewritten as

$$r\left(t\right) = s\left(t\right) * h\left(t\right) + n\left(t\right) \tag{6}$$

where $s(t)$ is the transmitted signal, and $h(t)$ is the channel impulse response which can be expressed as

$$h\left(t,\theta\right) = \sum_{k=1}^{K} \sum_{l=1}^{L_k} \mu_{kl} \delta\left(t - T_k - \tau_{kl}\right) \delta\left(\theta - \theta_k - \omega_{kl}\right) \tag{7}$$

where $\delta(.)$ is the dirac-delta function, K is the number of clusters, L_k is the number of rays in the k^{th} cluster, and μ_{kl}, τ_{kl} and ω_{kl} denote the complex amplitude, delay and azimuth of the k^{th} ray of the l^{th} cluster, respectively. Similarly, T_k and θ_k represent the delay and mean Angle of Arrival (AOA) of the k^{th} cluster.

2.4. Energy Detector

After the amplifier, the received signals are squared, and then input to an integrator with integration period Tb. Because of the inter-frame leakage due to multipath signals, the integration duration is $3T_f / 2$, so the number of signal values for energy detector is

$N = 3T_f / 2Tb$. The integrator outputs can be expressed as:

$$z[n] = \sum_{i=1}^{N} \int_{(i-1)T_f + (c_j + n)Tb}^{(i-1)T_f + (c_j + n - 1)Tb} r^2(t)dt \tag{8}$$

where $n \in \{1, 2, .., N\}$ denotes the sample index with respect to the starting point of the integration period and N is the number of pulses per symbol. Here, N is set to 1, so the integrator outputs are

$$z[n] = \sum_{i=1}^{N} \int_{(c_j + n)Tb}^{(c_j + n - 1)Tb} r^2(t)dt \tag{9}$$

If $z[n]$ is the integration of noise only, it has a centralized Chi-square distribution, while it has a non-centralized Chi-square distribution if a signal is present. The mean and variance of the noise and signal values are given by [17] respectively.

$$\mu_0 = F\sigma^2, \sigma_0 = 2F\sigma^4 \tag{10}$$

$$\mu_e = F\sigma^2 + E_n, \sigma_e^2 = 2F\sigma^4 + 4\sigma^2 E_n \tag{11}$$

where E_n is the signal energy within the n^{th} integration period and F is the number of degrees of freedom given by $F = 2BTb + 1$. Here B is the signal bandwidth.

3. LOS/NLOS Identification

3.1. Description of the Parameters

In this paper, we distinguish between the LOS or NLOS scenarios by exploiting the statistics of the received signal by energy detector. The minimum slope and kurtosis of the energy block is used in order to identify the LOS and NLOS scenarios respectively.

The slope of the energy values is considered as a measure. These values are divided into (N-M+1) groups, with M values in each group. The slope for each group is calculated using a least squares line-fit. The minimum slope can then be expressed as

$$MS = \min_{1 \le n \le N - M + 1} slope\left\{linefit\left(z[n], z[n+1], ..., z[n+M-1]\right)\right\} \tag{12}$$

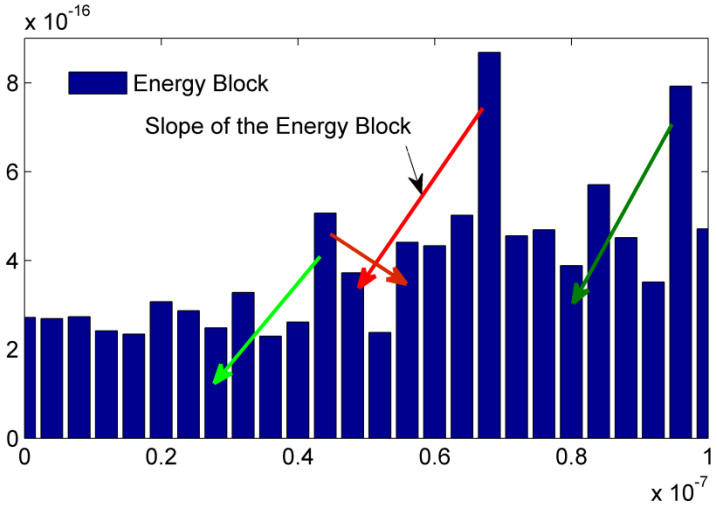

Figure 2. Slope of the Energy Block

The kurtosis is calculated using the second and fourth order moments and is given by

$$K = \frac{E\left[\left(x_i - \mu_x\right)^4\right]}{E\left[\left(x_i - \mu_x\right)^2\right]^2} = \frac{E\left[\left(x_i - \mu_x\right)^4\right]}{\sigma_x^4} \tag{13}$$

where μ_x is the mean value, and σ_x is the standard deviation. The kurtosis for a standard normal distribution is three. For this reason, kurtosis is often redefined as $K = K - 3$ (often referred to as "excess kurtosis"), so that the standard normal distribution has a kurtosis of zero, positive kurtosis indicates a "peaked" distribution and negative kurtosis indicates a "flat" distribution. For noise only (or for a low SNR) and sufficiently large *F* (degrees of freedom of the Chi-square distribution), $z[n]$ has a Gaussian distribution and kurtosis = 0. On the other hand, as the SNR increases, kurtosis will tend to increase.

3.2 Identification Approach

The ratio values of slope and kurtosis of the energy block can be obtained for both LOS and NLOS scenarios using sample channel realizations from both scenarios. Here, we used sample channel realizations of the IEEE 802.15.3c standard channel models in order to obtain the values of the slope of the energy slope for both LOS and NLOS.

In order to examine the characteristics of the ratio of kurtosis and minimum slope, the CM1.1 (residential LOS) and CM2.1 (residential NLOS) channel models from the IEEE802.15.3c standard are employed. For each SNR value, 1000 channel realizations are generated and sampled at $f_c = 1 \cdot e^{10}$ *Hz*. The other system parameters are $T_f = 200ns$, $T_c = 1ns$, the value of Tb is from 1 ns to 4 ns and *N*=1. Each realization has a TOA uniformly distributed within $\left(0 - T_f\right)$.

Here the SNR ranges from 0 dB to 7 dB, 1000 channel realizations are generated for each SNR. The CM1.1 (residential LOS) and CM2.1 (residential NLOS) channel models from the IEEE802.15.3c standard are employed. Here are 8*1000 samples which are got for each channel model. The relationship between Minimum Slope and SNR are shown in Figures 3-6.

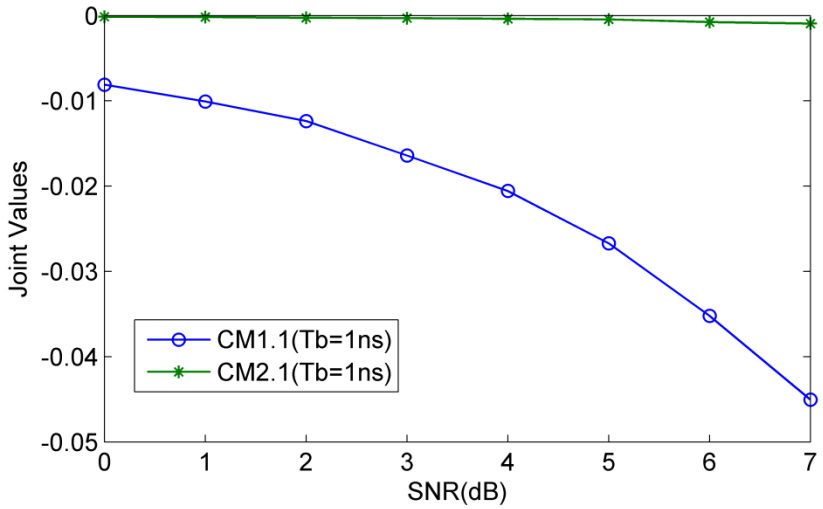

Figure 3. Joint Values with Respect to SNR (CM1.1 and CM2.1 with Tb=1ns)

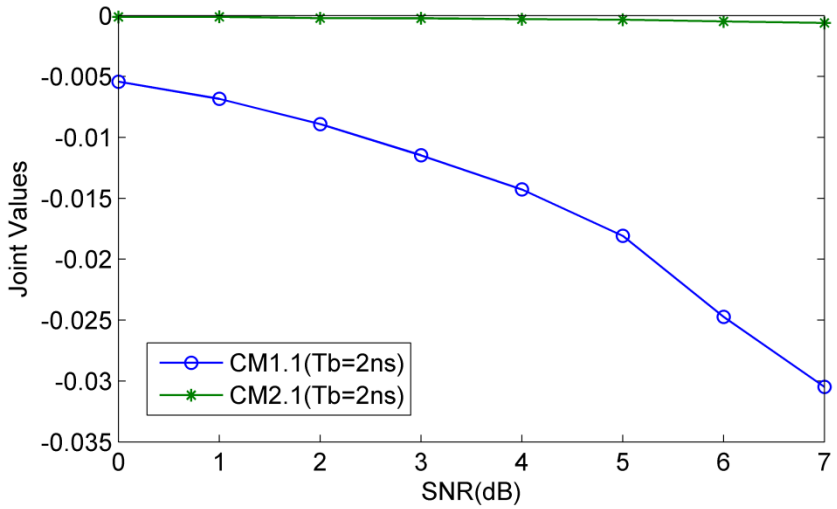

Figure 4. Joint Values with Respect to SNR (CM1.1 and CM2.1 with Tb=2ns)

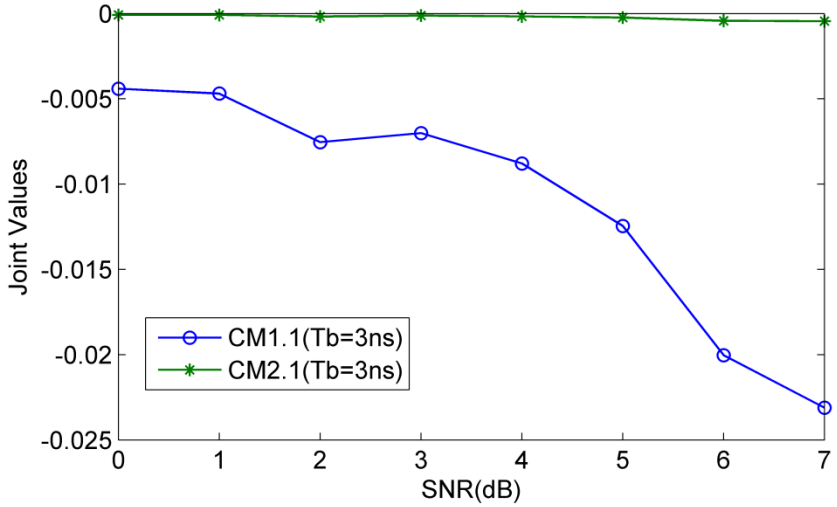

Figure 5. Joint Values with Respect to SNR (CM1.1 and CM2.1 with Tb=3ns)

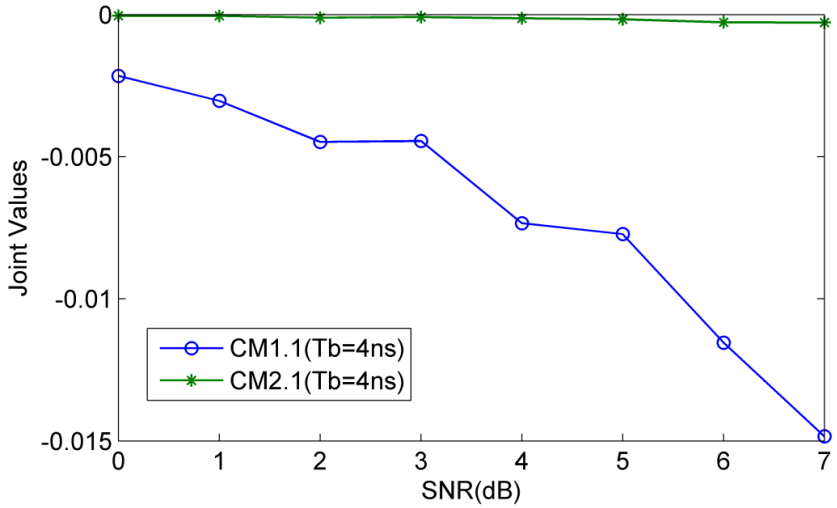

Figure 6. Joint Values with Respect to SNR (CM1.1 and CM2.1 with Tb=4ns)

From Figures 3-6, results show that the ratio values of minimum slope and kurtosis is monotonous with respect to SNR (both LOS and NLOS environment) in the 60 GHz wireless communication system respectively. But we find maximum of joint values (LOS) is even less than minimum of joint values (NLOS) when *TX* is 360, minimum of joint values (LOS) is even larger than maximum of joint values (NLOS) when *TX* is others. So we propose a novel method to identify the LOS and NLOS which can be expressed as:

$$\Theta = \alpha \begin{cases} \begin{cases} < \alpha_{MS} \Rightarrow LOS \\ > \alpha_{MS} \Rightarrow NLOS \end{cases} & TX = 360^{\circ} \\ \begin{cases} < \alpha_{MS} \Rightarrow NLOS \\ > \alpha_{MS} \Rightarrow LOS \end{cases} & TX < 360^{\circ} \end{cases} \tag{14}$$

where α_{MS} is the threshold which is chosen to identify the LOS and NLOS, *TX*, *RX* is the beam-width of measured transmitter and receiver antenna respectively. Aiming at the ranges [A, B] dB for SNR, α_{MS} can be shown as follows :

$$\alpha_{MS} = -\max \left\{ \begin{matrix} mean\left[find\left(P\left(abs(MS) < \Theta_1 |_A \right) \geq \Phi \right) \right] \\ mean\left[find\left(P\left(abs(MS) < \Theta_2 |_B \right) \geq \Phi \right) \right] \end{matrix} \right\} \tag{15}$$

where Θ_1 and Θ_2 are threshold which meet the condition $P(MS > \Theta) \geq \Phi$ where SNR is upper and lower limits. Φ is the probability value which is required for choosing suitable threshold for NLOS identification. As shown in Figure 7, the distribution of K/M samples larger than a certain threshold value Θ for the IEEE802.15.3c channel. When Θ is set to be 1 and more than 950 of the 1000 K/M samples are distributed less than Θ . In the process of simulation, results show that if we use those samples whose probability distribution is high, we can guarantee accuracy of NLOS identification and remove some extreme values at the same time. Without loss of generality, here Φ is set to be 0.85.

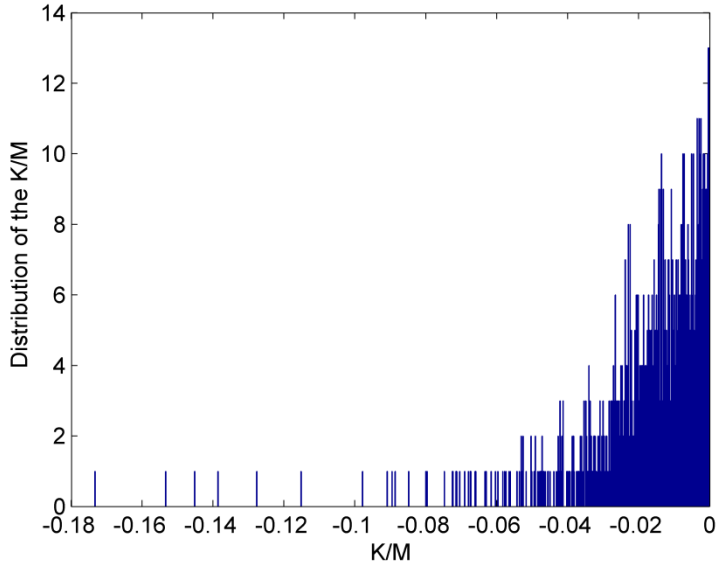

Figure 7. Distribution of the K/M

In order to verify the effectiveness and practicality of the algorithm, so we make a lot of simulations using IEEE 802.15.3c channel models. The CM1.2, CM1.3, CM1.4 (residential LOS) and CM2.2, CM2.3, CM2.4 (residential NLOS) channel models from

the IEEE802.15.3c standard are employed. For each SNR value, 1000 channel realizations are generated and sampled at $f_c = 1 \cdot e^{10}$ Hz. The other system parameters are $T_f = 200ns$, $T_c = 1ns$, the value of Tb is from 1ns to 4ns and N = 1. Each realization has a TOA uniformly distributed within $\left(0 - T_f\right)$.

Here the SNR ranges from 0 dB to 7 dB, 1000 channel realizations are generated for each SNR. The CM1.2, CM1.3, CM1.4 (residential LOS) and CM2.2, CM2.3, CM2.4 (residential NLOS) channel models from the IEEE802.15.3c standard are employed. Here are 8*1000 samples which are got for each channel model. The relationship between joint parameter and SNR are shown in Figures 8-19.

In order to verify the effectiveness of the NLOS identification algorithm, 1000 channel realizations were generated when SNR is from 0 dB to 7 dB in each IEEE802.15.3c channel and other system parameters as above. The threshold values and accuracy for identifying LOS and NLOS were calculated for each IEEE802.15.3c channel model. As shown in Table 2, accuracy increases for LOS environment and decreases for NLOS environment as the SNR increases when $TX = 360$. Conversely, accuracy increases for NLOS environment and decreases for LOS environment as the SNR increases when $TX < 360$. Accuracy of LOS/NLOS identification is higher than any other identification algorithms based on energy detect such as in [21], the accuracy is only around 60% while the accuracy of the proposed algorithm over 70% for most channel model.

Table 2. Threshold Values for LOS and NLOS Identification

Channel Model	2(dB)	3(dB)	4(dB)	5(dB)	6(dB)	Mean Values
CM1.1	39.0	47.5	57.6	62.3	70.6	55.40
CM2.1	78.9	74.4	71.9	67.5	61.9	70.92
CM1.2	92.7	87.1	78.6	66.2	59.3	76.78
CM2.2	83.3	87.1	88.5	91.2	92.1	88.44
CM1.3	89.7	84.8	79.0	68.4	57.3	75.84
CM2.3	97.0	98.2	97.6	98.5	98.7	98.00
CM1.4	91.9	88.2	80.2	69.5	60.3	78.02
CM2.4	95.2	97.2	95.9	97.6	98.0	96.78

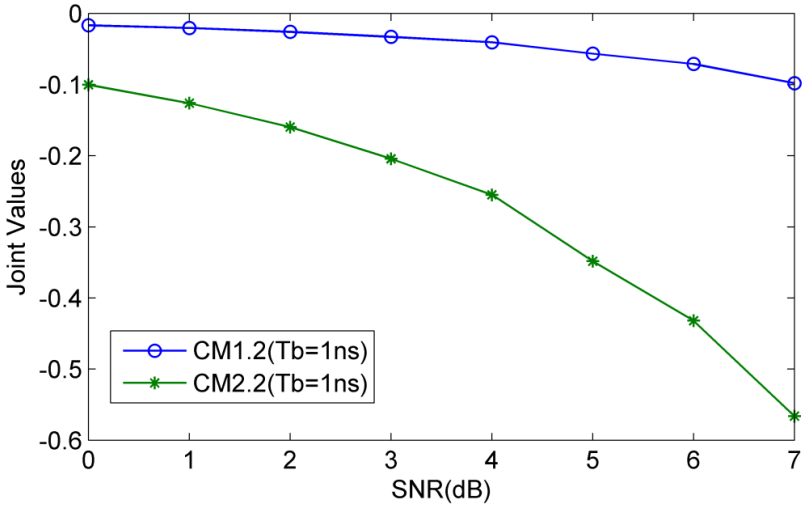

Figure 8. Joint Values with Respect to SNR (CM1.2 and CM2.2 with Tb=1ns)

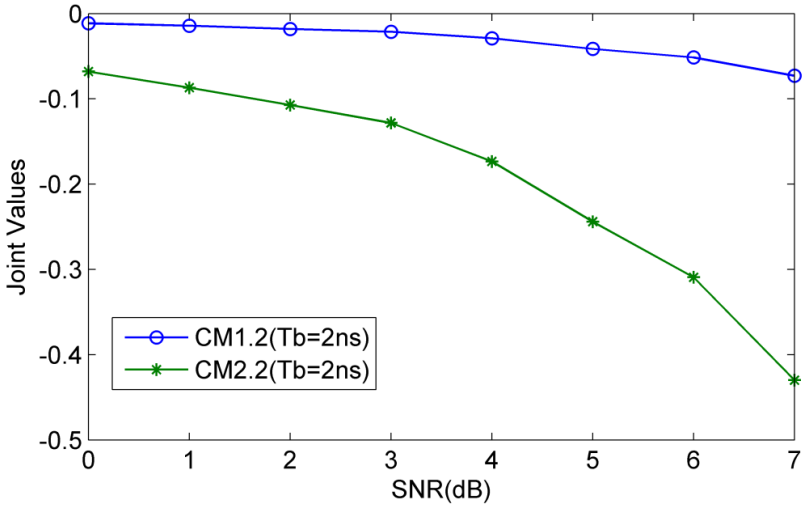

Figure 9. Joint Values with Respect to SNR (CM1.2 and CM2.2 with Tb=2ns)

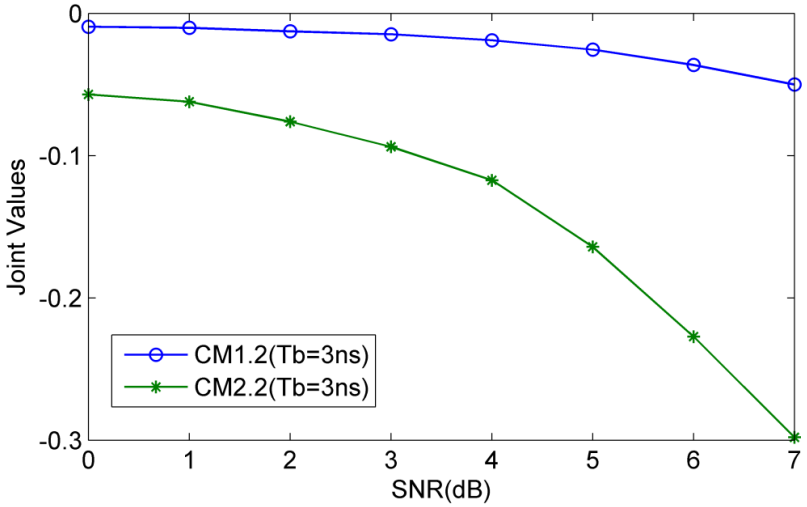

Figure 10. Joint Values with Respect to SNR (CM1.2 and CM2.2 with Tb=3ns)

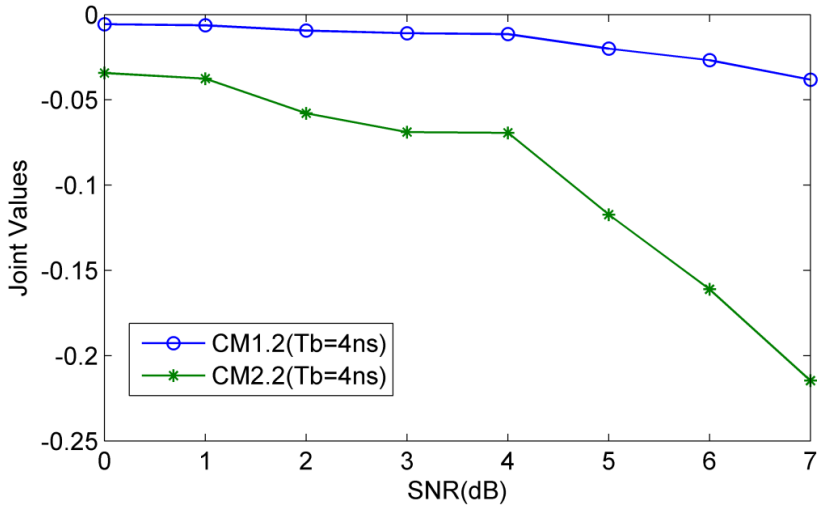

Figure 11. Joint Values with Respect to SNR (CM1.2 and CM2.2 with Tb=4ns)

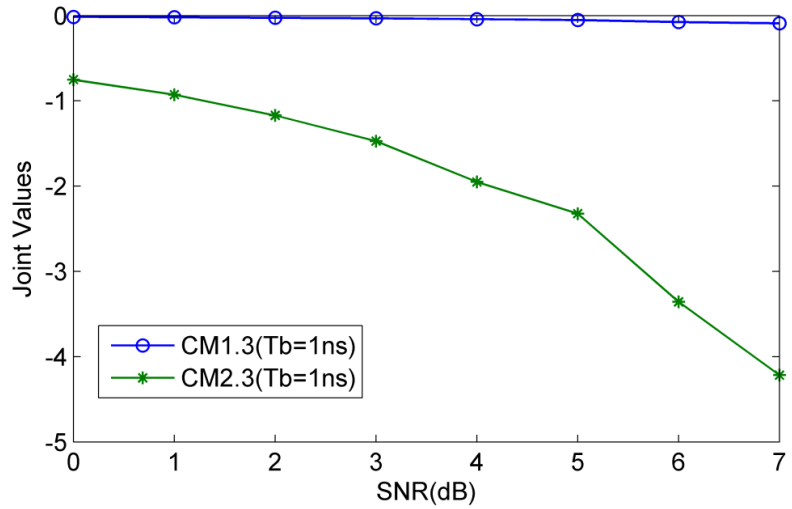

Figure 12. Joint Values with Respect to SNR (CM1.3 and CM2.3 with Tb=1ns)

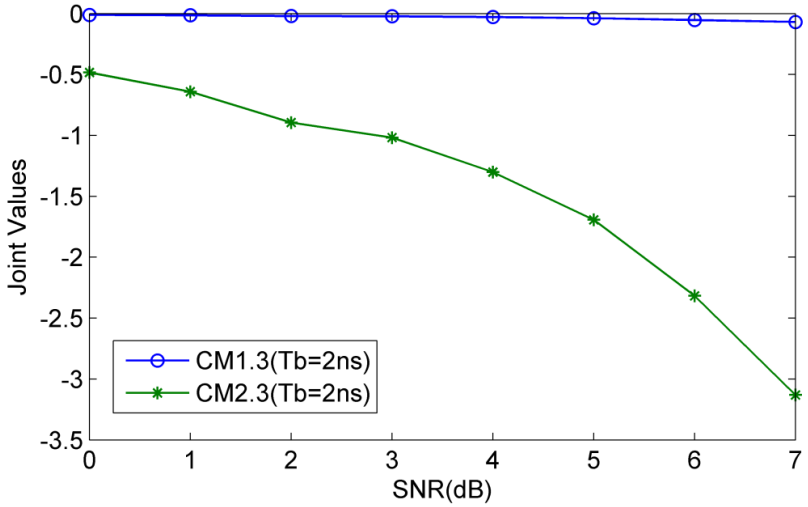

Figure 13. Joint Values with Respect to SNR (CM1.3 and CM2.3 with Tb=2ns)

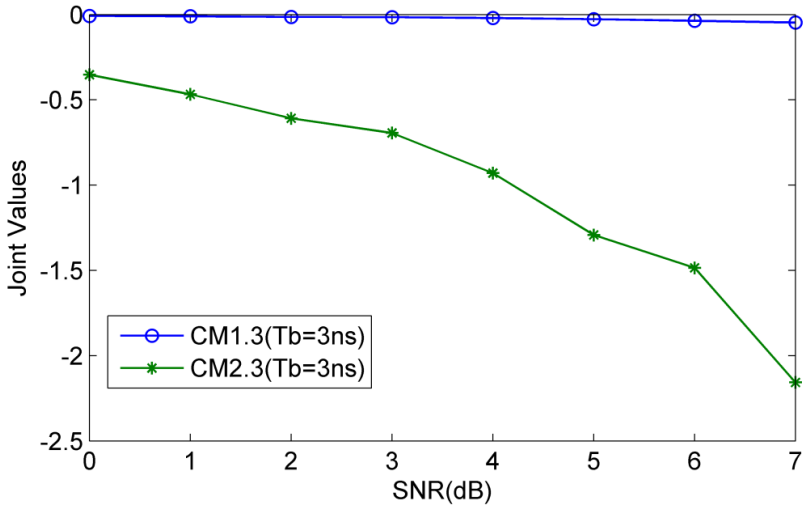

Figure 14. Joint Values with Respect to SNR (CM1.3 and CM2.3 with Tb=3ns)

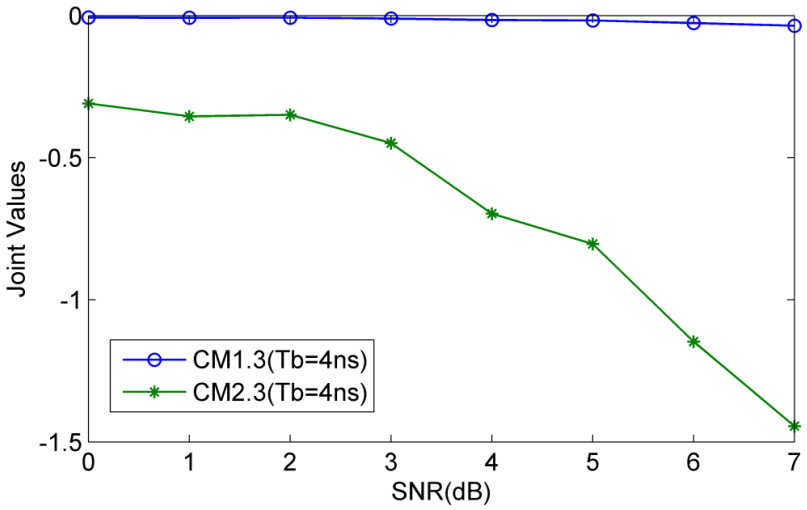

Figure 15. Joint Values with Respect to SNR (CM1.3 and CM2.3 with Tb=4ns)

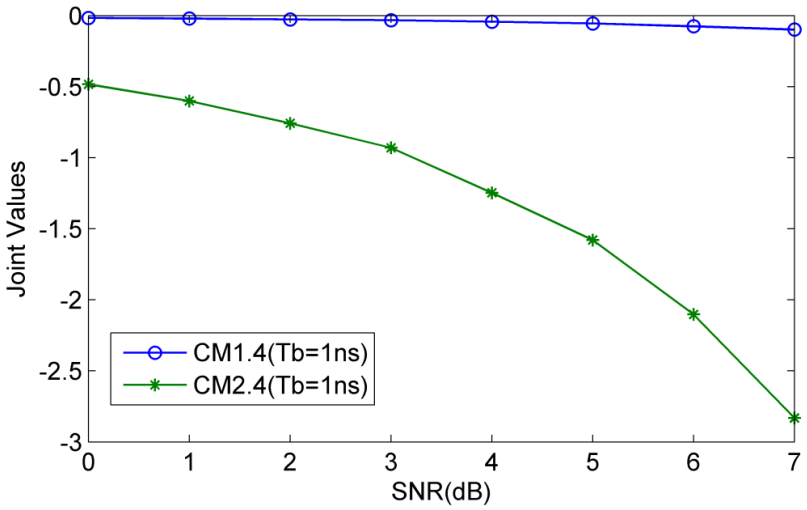

Figure 16. Joint Values with Respect to SNR (CM1.4 and CM2.4 with Tb=1ns)

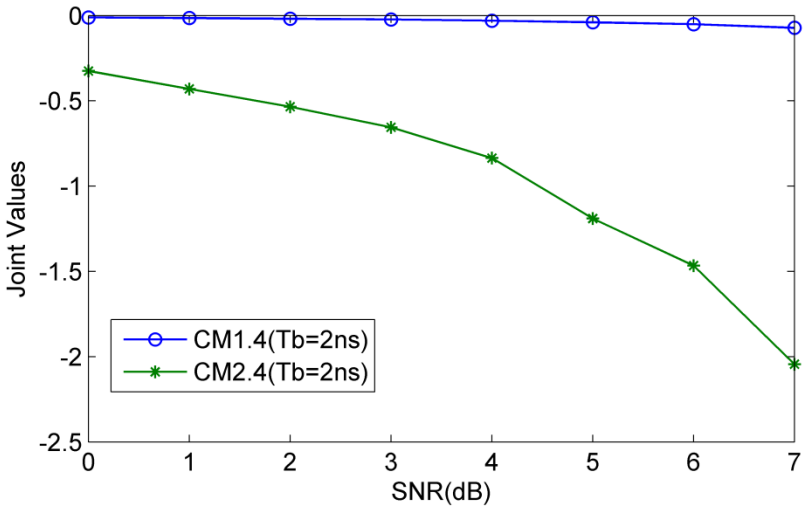

Figure 17. Joint Values with Respect to SNR (CM1.4 and CM2.4 with Tb=2ns)

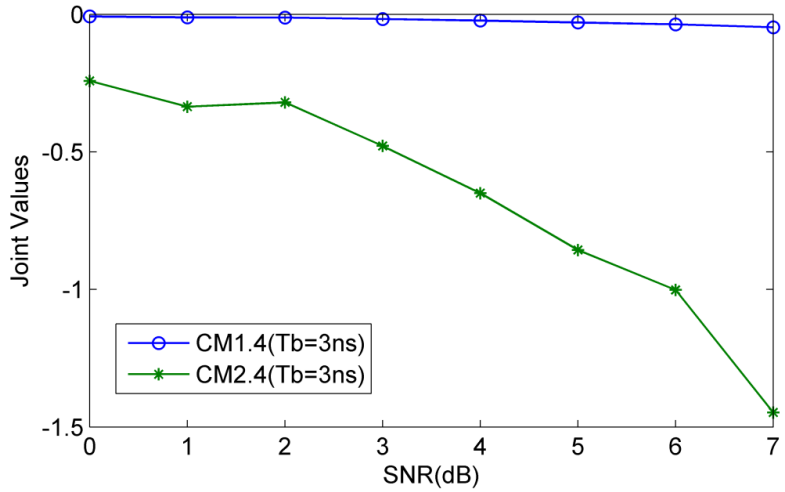

Figure 18. Joint Values with Respect to SNR (CM1.4 and CM2.4 with Tb=3ns)

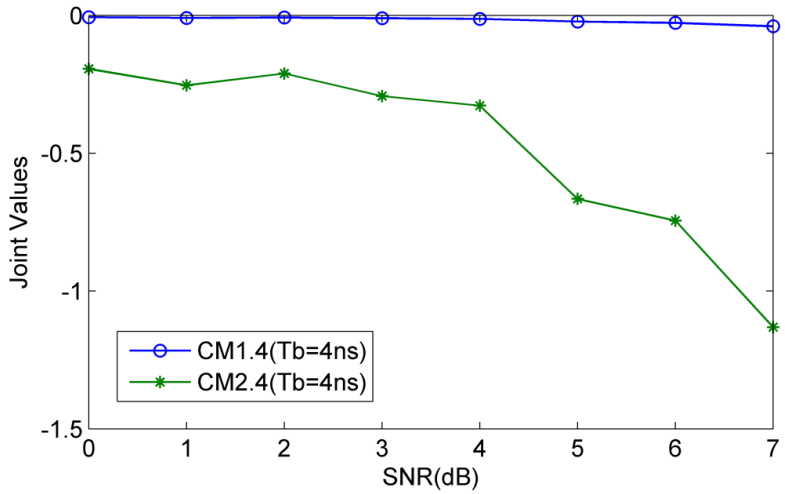

Figure 19. Joint Values with Respect to SNR (CM1.4 and CM2.4 with Tb=4ns)

From Figures 8-19, results show that joint parameter can identify the LOS and NLOS environments so long as the threshold α_{MS} can be fixed better.

4. Conclusion

In this paper, we presented a novel approach to deal with NLOS propagation that relies solely on features extracted from the received waveform. This technique does not require formulation of explicit statistical models for the features which is based on the minimum slope and kurtosis of energy block of the received signal using energy detector.

In order to verify the effectiveness and practicality of the algorithm, so we make a lot of simulations using IEEE 802.15.3c channel models. The CM1.1, CM1.2, CM1.3, CM1.4 (residential LOS) and CM2.1, CM2.2, CM2.3, CM2.4 (residential NLOS) channel models from the IEEE 802.15.3c standard are employed. Results show that the joint parameter can identify the LOS and NLOS environments so long as the threshold α_{MS} can be fixed bitterly.

We developed techniques that are capable of distinguishing LOS/NLOS propagation in NLOS conditions. Our results revealed that the proposed technique outperforms previous parametric techniques from the literature. But here is a question that the method we

proposed can't identify the LOS and NLOS environments in the office. So in the future, this will be the problem which is eager to be solved for us.

Acknowledgments

The authors would like to thank colleagues from the UWB Laboratory in the College of Information Science and Engineering, Ocean University of China, for help with obtaining the measurement data. This work was supported by the Nature Science Foundation of China under Grant No. 60902005, the Qingdao International Science and Technology Cooperation Projects of Qingdao under Grant No. 12-1-4-137-hz, the Nature Science Foundation of China under Grant No. 61301139, the Nature Science Foundation of Shandong Province under Grant No. ZR2014FL014, the Science and Technology Project in Colleges and Universities of Shandong Province under Grant No.J14LN53, the Project of Basic Research Application of Qingdao City under Grant No. 14-2-4-37-jch, and the Project of Basic Research Application of Qingdao City under Grant No. 14-2-4-83-jch.

Reference

[1] L. Zhang, "A fully integrated 60GHz four channel CMOS receiver with 7GHz ultra-wide band width for IEEE 802.11ad standard", Communication, China, vol. 11, no. 6, **(2014)**, pp. 42-50.
[2] S. K. Yong and C. C. Chong, "An overview of multi gigabit wireless through millimeter Wave Strategy: Potentials and Technical Challenges", EURASIP J. Wireless Communications and Networking, vol. 2007, no. 1, **(2007),** pp. 1-10.
[3] R. C. Daniels and R. W. Heath, "60 GHz wireless communications: emerging requirements and design recommendations", IEEE Vehicular Strategy Society, vol. 2, **(2007),** pp. 41-50.
[4] C. C. Chong, F. M. Peter, Smulders, "60GHz-Millimeter-Wave Radio Principle, Strategy, and News Results", EURASIP Journal on Wireless Communications and Networking, vol. 2007, no. 1, **(2007)**, pp. 1-8.
[5] S. K. Yong, P. F. Xia and V. G. Alberto, "60-GHz Strategy for Gbps WLAN and WPAN: From Theory to Practice", Beijing: Press of China Machine, **(2013).**
[6] R. C. Daniels and R. W. Health, "60 GHz wireless communications: emerging requirements and design recommendations", IEEE Vehicular Strategy Magazine, vol. 2, no. 3, **(2007),** pp. 41-50.
[7] M. P. Wylie and J. Holtzman, "The non-line of sight problem in mobile location estimation," in Proceedings of the 5th IEEE International Conference on Universal Personal Communications (ICUPC '96), Cambridge, Mass,USA, September-October , vol. 2, **(1996)**, pp. 827–831,
[8] J. Borras, P. Hatrack and N. B. Mandayam, "Decision theoretic framework for NLOS identification," in Proceedings of the 48th IEEE Vehicular Technology Conference (VTC '98), Ottawa, Canada, vol. 2, May **(1998)**, pp. 1583–1587,
[9] I. Guvenc, C-C. Chong and F. Watanabe, "NLOS identification and mitigation for UWB localization systems", Wireless Communications and Networking Conference, 2007. WCNC. IEEE, **(2007)**, pp. 1571–1576.
[10] M. Heidari, F.O. Akgul and K. Pahlavan, "Identification of the absence of direct path in indoor localization systems", IEEE International Symposium on Personal, Indoor, and Mobile Radio Communications, **(2007)**, pp. 1–6
[11] S. Venkatesh and R.M. Buehrer, "Non-line-of-sight identification in ultra-wideband systems based on received signal statistic", Microwaves, Antennas & Propagation, IET, vol. 1, no. 6, **(2007)**, pp. 1120–1130.
[12] H Shimizu, H Masui, M Ishii and K Sakawa, "LOS and NLOS path-loss and delay characteristics at 3.35 GHz in a residential environment", Antennas and Propagation Society International Symposium, 2000. IEEE, vol. 2, **(2000)**, pp. 1142–1145.
[13] I. Güvenç, C-C Chong, F. Watanabe and H. Inamura, "NLOS identification and weighted least-squares localization for UWB systems using multipath channel statistics", EURASIP Journal on Advances in Signal Processing, 14 Article ID 271984, **(2008)**.
[14] "IEEE Standard for Information strategy--Local and metropolitan area networks--Specific requirements--Part 15.3: Wireless Medium Access Control (MAC) and Physical Layer (PHY) Specifications for High Rate Wireless Personal Area Networks (WPAN) amendment 2: millimeter-wave-based alternative physical layer extension". IEEE Computer Society, IEEE 802.15.06-0474-00-003c. New York, USA, **(2009).**
[15] "802.11n-2009-IEEE Standard for Information strategy-- Local and metropolitan area networks--Specific requirements--Part 11: Wireless LAN Medium Access Control (MAC)and Physical Layer (PHY) Specifications Amendment 5: Enhancements for Higher Throughput", IEEE Computer

Society, IEEE 978-0-7381-6731-2. New York, USA, **(2009).**
[16] C. R. Andersonn and T. S. Rappaport, "In-building wideband partition loss measurements at 2.5 and 60GHz", IEEE Transactions on Wireless Communications, vol. 3, no. 3, **(2004),** pp. 922-928.
[17] S. Collong, G. Zaharia and G. E. Zein, "Influence of the human activity on wide-band characteristics of the 60GHz indoor radio channel", IEEE Transactions on Wireless Communications, vol. 3, no. 6, **(2005)**, pp. 2396-2406.
[18] A. Maltsev, R. Maslennikov and A. Sevastyanov, "Experimental investigations of 60GHz WLAN systems in office environment", IEEE Journal on Selected Areas in Communications, vol. 27, no. 8, **(2009)**, pp. 1488-1499.
[19] M. G. Sanchez, A. V. Alejos and I. Cuinas, "Comparision of space diversity performance in indoor radio channels at 40GHz and 60GHz", Proc. of European Conference on Wireless Strategy, Amsterdam, **(2008).**
[20] H. B. Yang, "Channel characteristics and transmission performance for various channel configurations at 60GHz", EURASIP Journal on Wireless Communications and Networking, vol. 2007, no. 1, **(2007)**, pp. 43-43.
[21] S. H. WU, Q. Y. Zhang and N. T. Zhang, "NLOS Identification for IR-UWB Ranging Systems", Journal of Electronics & Information Technology ,vol. 30, no. 11, **(2008)**, pp. 2541-2546.

Authors

Xiaolin Liang now studies in College of Information Science and Engineering and is a Ph. D. candidate in Ocean University of China. His research interests include ultra-wideband radio systems, 60 GHz wireless communication system.

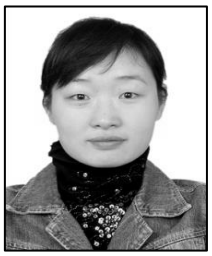

Tingting Lu received the Ph. D. degree in College of Information Science and Engineering from Ocean University of China in 2013. She is now a lecture in College of Information Science and Engineering. Her research interests include ultra-wideband radio systems, 60 GHz wireless communication system.

Hao Zhang received the MBA degree in New York Institute of Technology, American in 2001 and the Ph. D. degree in Electrical and Computer Engineering from the University of Victoria, Canada in 2004. He was a Project Manager for Microsoft Inc. in United States during January 2000-May 2000. During 2004-2008, he was the Vice President for the United States Gamma Capital Inc. He is now an Adjunct Assistant Professor in the Department of Electrical and Computer Engineering. Also he becomes a professor and the Ph. D. supervisor in College of Information Science and Engineering from Ocean University of China in 2006. His research concerns ultra-wideband radio systems, 60 GHz wireless communication system and MIMO wireless communication.

T. Aaron. Gulliver received the Ph. D. degree in Electrical and Computer Engineering from the University of Victoria, Canada in 1989. He is now a professor and the Ph. D. supervisor in the Department of Electrical and Computer Engineering. In 2002, he becomes a Fellow of the Engineering Institute of Canada, and in 2012 a Fellow of the Canadian Academy of Engineering. He is also a senior member of IEEE. His research concerns information theory and communication theory, algebraic coding theory and smart grid and ultra wideband communication.